Deconstructing *Methanosarcina acetivorans* into an acetogenic archaeon

Christian Schöne[a], Anja Poehlein[b], Nico Jehmlich[c], Norman Adlung[d], Rolf Daniel[b], Martin von Bergen[c], Silvan Scheller[d], and Michael Rother[a,1]

[a]Institute of Microbiology, Technische Universität Dresden, 01062 Dresden, Germany; [b]Institute of Microbiology and Genetics, Georg-August-Universität Göttingen, 37077 Göttingen, Germany; [c]Department of Molecular Systems Biology, Helmholtz Centre for Environmental Research, 04318 Leipzig, Germany; and [d]Department of Bioproducts and Biosystems, Aalto University, 02150 Espoo, Finland

Edited by Mary Lidstrom, Office of Research, University of Washington, Seattle, WA; received July 27, 2021; accepted November 16, 2021

The reductive acetyl-coenzyme A (acetyl-CoA) pathway, whereby carbon dioxide is sequentially reduced to acetyl-CoA via coenzyme-bound C1 intermediates, is the only autotrophic pathway that can at the same time be the means for energy conservation. A conceptually similar metabolism and a key process in the global carbon cycle is methanogenesis, the biogenic formation of methane. All known methanogenic archaea depend on methanogenesis to sustain growth and use the reductive acetyl-CoA pathway for autotrophic carbon fixation. Here, we converted a methanogen into an acetogen and show that *Methanosarcina acetivorans* can dispense with methanogenesis for energy conservation completely. By targeted disruption of the methanogenic pathway, followed by adaptive evolution, a strain was created that sustained growth via carbon monoxide–dependent acetogenesis. A minute flux (less than 0.2% of the carbon monoxide consumed) through the methane-liberating reaction remained essential, indicating that currently living methanogens utilize metabolites of this reaction also for anabolic purposes. These results suggest that the metabolic flexibility of methanogenic archaea might be much greater than currently known. Also, our ability to deconstruct a methanogen into an acetogen by merely removing cellular functions provides experimental support for the notion that methanogenesis could have evolved from the reductive acetyl-coenzyme A pathway.

Methanosarcina | methanogenic | acetogenic | acetyl-CoA pathway

The reduction of two carbon dioxide (CO_2) to an activated acetyl group using inorganic electron donors, the reductive acetyl-coenzyme A (acetyl-CoA) pathway, is considered to be (among) the oldest metabolism(s), its reaction principles possibly predating the genes for the enzymes involved (1–3). It is the only metabolic pathway that can be involved both in carbon fixation and energy conservation. In the bacterial domain, the reductive acetyl-CoA pathway involves tetrahydrofolate (H_4F) as the major one-carbon transferring cofactor (4) and hydrolysis of ATP for the activation of CO_2 to formyl-H_4F (5). Energy conservation through this cytoplasmic pathway can be achieved via membranous oxidoreductases generating an ion motive force (6). In contrast, members of the archaeal domain employ a variant of the pathway that involves tetrahydromethanopterin (H_4MPT) (7) and either flavin-based electron bifurcation or reverse electron transfer for the activation of CO_2 to formyl-H_4MPT (via formyl-methanofuran, *SI Appendix*, Fig. S1) (8). The archaeal acetyl-CoA pathway is mostly employed for carbon assimilation (9, 10). Only *Archaeoglobus fulgidus* and *Methanosarcina acetivorans* were shown to use this pathway for energy conservation by acetogenic carbon monoxide utilization (11, 12). As of yet uncultivated Archaea are suspected to grow acetogenically based on their genetic inventory (13–15).

A globally important archaeal energy metabolism is methanogenesis. It shares reactions with the reductive acetyl-CoA pathway but lacks the carbonyl and extends the methyl branch (Fig. 1). This extension encompasses 1) the exergonic transfer of the H_4MPT-bound methyl group to 2-mercaptoethanesulfonate (coenzyme M, HS-CoM) by the membrane-integral, sodium-dependent (i.e., energy-converting) N^5-methyl-H_4MPT:HS-CoM methyltransferase (Mtr) (16), which generates a sodium motive force; 2) the reduction of methyl-S-CoM to methane, catalyzed by methyl-S-CoM reductase (Mcr) (17) using 7-mercaptoheptanoylthreonine phosphate (coenzyme B, HS-CoB) as a reductant; and 3) the reduction of the resulting heterodisulfide, CoM-S-S-CoB, by heterodisulfide reductase (Hdr) (Fig. 1). The last archaeal common ancestor was proposed to have been a methanogen (18–20), which seems counterintuitive considering that all autotrophic methanogens use the reductive acetyl-CoA pathway for carbon fixation and that the methanogenic "extension" of the methyl branch involves additional enzymes (the Mtr-Mcr-Hdr "module," Fig. 1) and sophisticated catalysis (the Mcr reaction has currently no precedence in laboratory chemistry) as well as an unusual principle of energetic coupling (generation of a sodium motive force by methyl transfer) (21). Despite the acetogenic lifestyle being not well documented for extant Archaea, evolving the methanogenic trait from an acetogenic ancestor seems plausible. In this communication, we deconstructed (i.e., simplified) *Methanosarcina acetivorans*, a member of the methanogenic Euryarchaeota, into an acetogen. Previous analyses showed that growth of *M. acetivorans* on carbon monoxide (CO) coincides with an approximate eightfold reduction (as compared to Methanol as substrate) in abundance of energy-converting Mtr

Significance

The reductive acetyl-coenzyme A (acetyl-CoA) pathway is the only carbon fixation pathway that can also be used for energy conservation like it is known for acetogenic bacteria. In methanogenic archaea, this pathway is extended with one route toward acetyl-CoA formation for anabolism and another route toward methane formation for catabolism. Which of these traits is ancestral in evolution has not been resolved. By diverging virtually all substrate carbon from methanogenesis to flow through acetyl-CoA, *Methanosarcina acetivorans* can be converted to an acetogenic organism. Being able to deconstruct methanogenic into the seemingly simpler acetogenic energy metabolism provides compelling evidence that methanogens are not nearly as metabolically limited as previously thought and suggests that methanogenesis might have evolved from the acetyl-CoA pathway.

Author contributions: C.S., S.S., and M.R. designed research; C.S., A.P., N.J., and N.A. performed research; C.S., A.P., N.J., N.A., R.D., M.v.B., S.S., and M.R. analyzed data; and C.S., A.P., N.J., N.A., R.D., M.v.B., S.S., and M.R. wrote the paper.

The authors declare no competing interest.

This article is a PNAS Direct Submission.

[1]To whom correspondence may be addressed. Email: michael.rother@tu-dresden.de.

This article contains supporting information online at http://www.pnas.org/lookup/suppl/doi:10.1073/pnas.2113853119/-/DCSupplemental.

Published January 6, 2022.

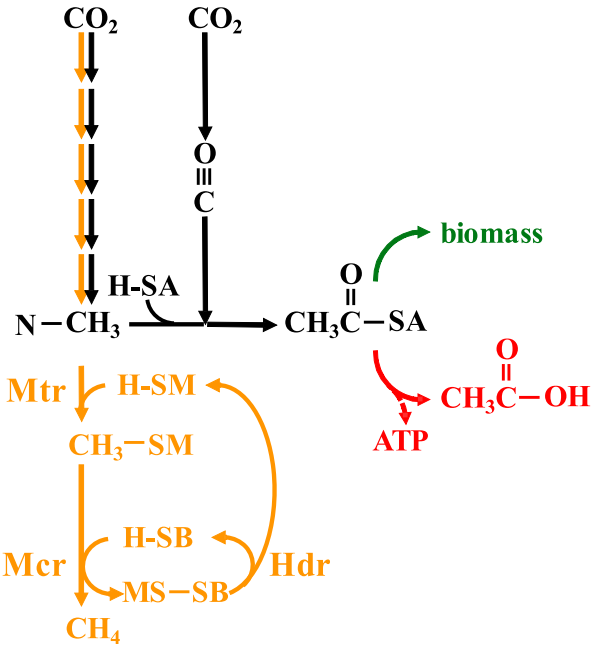

Fig. 1. The acetyl CoA pathway and methanogenesis. Whether H_4F or H_4MPT is the pterin cofactor (-N) in the methyl branch of the acetyl-CoA pathway (black) is not indicated; activated acetyl group is either used anabolically (green) or catabolically (red); methanogenesis (orange), reduction of methyl-N to methane involves Mtr (N^5-methyl-H_4MPT:HS-CoM methyltransferase), Mcr (methyl-S-CoM reductase), and Hdr (heterodisulfide reductase); for simplicity, thiol-containing cofactors coenzyme A, B, and M are abbreviated, and the input of electrons is not shown.

(22). After the removal of the Mtr-encoding genes (i.e., disruption of the methyl branch toward methane, Fig. 1), an *M. acetivorans* strain was selected, which grows in a sustained fashion acetogenically on CO. Despite this dramatic change of physiology, Mcr remained essential in the strain, most likely because of the requirement of the CoM-S-S-CoB heterodisulfide in at least one unknown essential anabolic reaction. The requirement of methanogenesis can, thus, be independent from energy conservation for *M. acetivorans*, which could represent a transition state in the evolution of an acetogenic into a methanogenic archaeon.

Results

Removing Mtr Leads to "Methyl Auxotrophy" in *M. acetivorans*. In order to create physiological reference data, the carboxidotrophic characteristics of *M. acetivorans* strain M42, used as wild type in this study, were assessed prior to mutagenesis (Fig. 2*A*). M42 converts more than 75% of the CO supplied to acetate (4 CO consumed per acetate produced) and less than 10% to methane (4 CO consumed per methane produced) during growth (Fig. 2*A*), confirming that acetogenesis rather than methanogenesis is the major CO-dependent catabolic pathway under this condition (*SI Appendix*, Fig. S1) (11). To investigate whether the organism's catabolism can be shifted completely toward acetogenesis, the operon encoding Mtr, *mtrEDCBAFGH* (MA0269-MA0276), was deleted from the chromosome (*SI Appendix*, Fig. S1) using a combination of CO and MeOH as energy substrates. The resulting mutant strain MKOmtr3 (*SI Appendix*, Table S1) was unable to grow on either MeOH or CO alone during 12 mo of incubation (*SI Appendix*, Table S2). While the requirement of Mtr during methylotrophic growth was expected (*SI Appendix*, Fig. S1), it was surprising that carboxidotrophic growth of MKOmtr3 was not possible considering its acetogenic potential (Fig. 2*A*).

MKOmtr3 did grow on a combination of acetate and methanol (Fig. 3*A*). The methanol concentrations required (Fig. 3 *A*, *Inset*) were substantial, which suggests that MKOmtr3 grew via methyl reduction like the corresponding *Methanosarcina barkeri* Δ*mtr* mutant (23). Under this condition, acetate serves as electron donor and methanol as electron acceptor (*SI Appendix*, Fig. S1). In contrast, growth on CO and methanol (the condition under which the mutant was isolated) required less than 2 mM MeOH for maximal yield (Fig. 3*B*), which rules out energy conservation of MKOmtr3 via methyl reduction, that is, methanogenesis. If exogenous methyl groups are essential for the CO-dependent growth of MKOmtr3 but not catabolic methanogenic substrates, most likely they were required for anabolic purposes. As MKOmtr3 quantitatively converted the methanol supplied to methane during CO-dependent growth (*SI Appendix*, Fig. S2), methyl-S-CoM, through which exogenous methyl groups are funneled toward central metabolism (24), could be ruled out as the required anabolic metabolite. The free thiols HS-CoM and HS-CoB are also unlikely candidates, as they would not get oxidized, that is, be present, in the absence of exogenous methyl groups. Instead, the CoM-S-S-CoB heterodisulfide appeared as the metabolite, most likely causing "methyl auxotrophy" in MKOmtr3.

Genetic Suppression Minimizes Methanogenesis. Next, attempts were made to replace the exogenous methyl groups with other reducible compounds that might allow generating CoM-S-S-CoB in a Mcr-independent fashion. Indeed, some of the reducible compounds tested (*SI Appendix*, Table S2) resulted in weak but visible growth of MKOmtr3. A concentration dependence could not be determined after the cultures had started to grow, that is, the cultures grew on CO alone. After 35 to 45 generations, the cell yield started to increase considerably, strongly suggesting that (a) spontaneous mutation(s), which suppressed

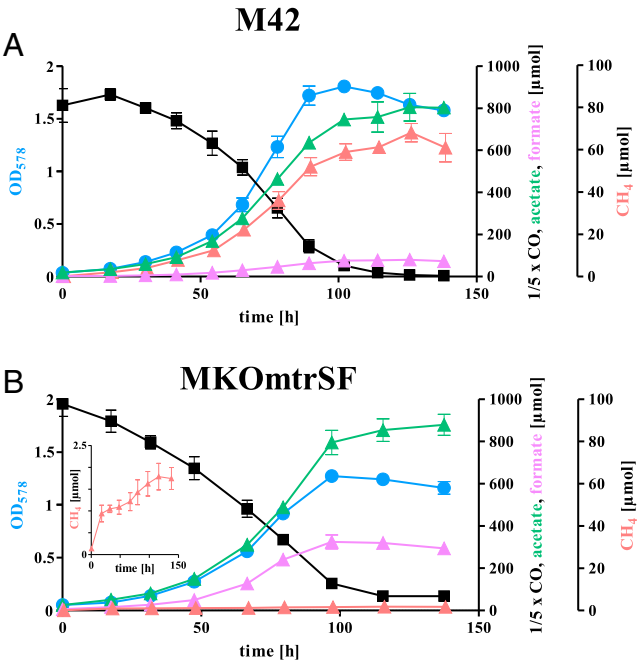

Fig. 2. Converting a methanogen into an acetogen. Biomass production (blue, OD_{578}), CO consumption (black, values have to be multiplied by 5 to get the actual amounts), and formation of acetate (green), formate (purple), and methane (red) in M42 (*A*, wild type) and MKOmtrSF (*B*, suppressor of *mtr* deletion, *SI Appendix*, Table S1) during carboxidotrophic growth. (*B*, *Inset*) Methane formation in a differently scaled *y*-axis; shown are mean values and their SDs (error bars) of 6 (M42) or 5 (MKOmtrSF) independent cultures (serum bottles), respectively; the result was reproduced twice.

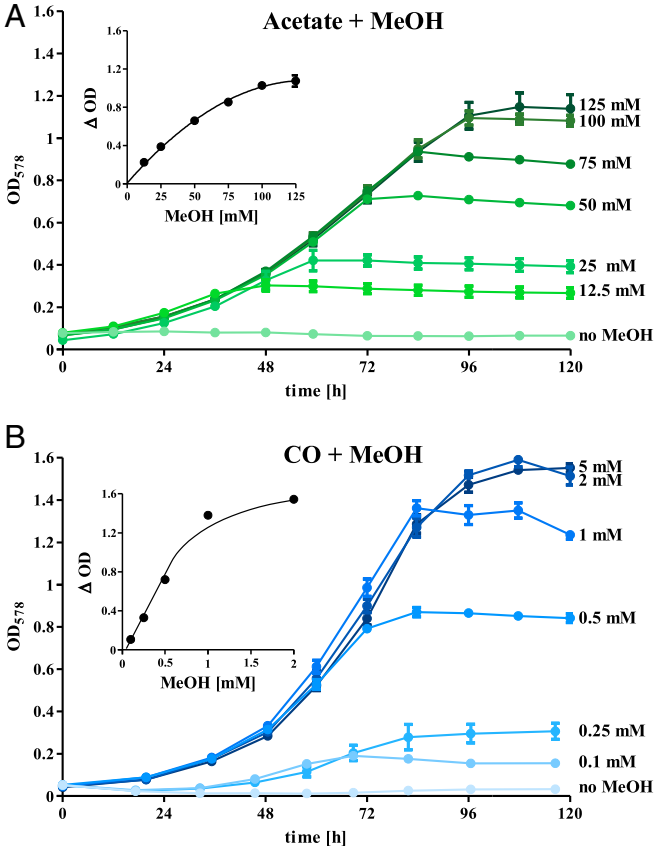

Fig. 3. Methyl reduction versus methyl group dependence in *M. acetivorans*. MKOmtr3 (lacking Mtr, *SI Appendix*, Table S1) could be grown on a combination of acetate (40 mM) and MeOH (*A*, Balch tubes) in which acetate oxidation drives methyl reduction to methane for energy conservation or of CO (150 kPa) and MeOH (*B*, serum bottles) in which CO-dependent acetogenesis serves energy conservation, while MeOH is required for anabolism. (*Insets*) Correlation of biomass yield (ΔOD, OD_{578} at the end of experiment minus OD_{578} at the beginning of experiment) and MeOH concentration supplemented; for each MeOH concentration, mean values and their SDs (error bars) of five independent cultures are shown.

the *mtr* phenotype (no growth on CO alone) and which had apparently also eliminated the requirement for the respective compound (*SI Appendix*, Table S2), had occurred and moved through the population. Clonal isolates of the potential suppressor mutants were obtained with CO as the sole energy source by picking single colonies from streaks on agar plates. One suppressor strain, obtained via initial supplementation with fumarate, was designated MKOmtrSF and investigated further.

MKOmtrSF grew on CO (Fig. 2*B*) very similarly to its parental strain MKOmtr3 (with MeOH added) in terms of growth rate, growth yield, and acetate and formate production (*SI Appendix*, Fig. S2). Methane formation, however, was almost completely abolished in MKOmtrSF (Fig. 2 *B*, *Inset*): less than 0.2% of the CO supplemented was converted to methane (i.e., more than 50-fold less than the wild type). Thus, spontaneous mutation has converted *M. acetivorans* to a CO-dependent acetogen.

According to the biomass yields, the energy metabolism of MKOmtrSF was somewhat diminished compared to the wild type (Table 1), which probably stems from losing Mtr as a coupling site. In nongrowing cell suspensions of both MKOmtr3 and MKOmtrSF, the balancing of metabolites produced from CO (methane, acetate, formate, and CO_2 were quantified) did not even out (*SI Appendix*, Table S3), suggesting both strains generate at least one unknown compound more reduced than CO (because of excess CO_2).

Shutting Off Methanogenic Respiration. To identify the mutation(s) that suppressed the *mtr* phenotype in MKOmtrSF and, thus, to unravel the basis for the dramatic change in physiology, its genome was (re)sequenced and compared to that of the wild type and of the parental strain MKOmtr3. All but one of the single nucleotide polymorphisms were present in all three strains (*SI Appendix*, Table S4) and are therefore not responsible for MKOmtrSF's phenotype. Unique to MKOmtrSF is a deletion of a threonine codon in MA1819, which encodes a homolog of AspB (25). Strikingly, MKOmtrSF also carries a 177,114-base pair lesion (compared to the reference strains), which corresponds to approximately 3% of its genome. From analyzing the sequences of the lesion's boundaries (*SI Appendix*, Fig. S3), no obvious mechanism for the deletion could be deduced. Whether any of the 159 open reading frames (*SI Appendix*, Table S5) deleted, an aberrant regulatory effect causing altered gene expression (five putative transcriptional regulators are encoded in the region missing, *SI Appendix*, Table S5), or the codon deletion in MA1819 (*SI Appendix*, Table S4) caused the phenotype of MKOmtrSF could not be unraveled, if only for the sheer number of genes affected.

To learn how the genomic changes of MKOmtrSF affected its protein inventory, it was compared to that of the wild type and to that of the parental strain MKOmtr3 through quantitative proteomic analysis. Of the predicted 4,660 proteins of *M. acetivorans* C2A (Reference Sequence Database NC_003552), 50 were differentially abundant (using a threshold of ± 2.5-fold) in MKOmtrSF compared to the wild type and 45 compared to its parental strain MKOmtr3 (*SI Appendix*, Table S6). Generally, removing Mtr in *M. acetivorans* led to increased abundance of proteins involved in methylotrophic metabolism (e.g., MtmC1, MtbA, RamA, MtpA, and MtsF, *SI Appendix*, Table S6), which may serve the purpose of making various sources of methyl groups accessible for the strain's "methyl auxotrophy" (*SI Appendix*, Fig. S2). A remarkable change in the proteome of the *mtr* suppressor MKOmtrSF compared to its parental strain was the decrease of proteins involved in methylotrophic metabolism (e.g., RamA, MtpCAP, MtsF, MtaC2B2, and five CobN homologs, *SI Appendix*, Table S6), lending support to the idea that a feature of *mtr* suppression is to reduce the capacity for methylotrophic metabolism.

The most striking proteomic feature of MKOmtrSF was that HdrD was absent (*SI Appendix*, Table S6). Together with HdrE, HdrD constitutes the terminal oxidoreductase of the respiratory chain of *Methanosarcina* species (8) (*SI Appendix*, Fig. S1). Consequently, MKOmtrSF essentially lacked membrane-associated Hdr activity (i.e., HdrED) (Fig. 4*A*). Thus, MKOmtrSF eliminates catabolic, that is, respiratory CoM-S-S-CoB reduction in order to grow acetogenically on CO. To confirm this conclusion, the HdrED-encoding genes (MA0687-MA0688) were deleted in MKOmtrSF (*SI Appendix*, Fig. S4). The resulting *hdrED* deletion mutant, designated MKOmtrhdr (*SI Appendix*, Table S1), displayed phenotypic characteristics very similar to those of its parental strain (Table 1, Fig. 2*B*, and *SI Appendix*, Fig. S4). Thus, the terminal oxidoreductase of the methanogenic respiratory chain, otherwise essential (26) for energy conservation (as a chemiosmotic coupling site) and for reduction of the CoM-S-S-CoB heterodisulfide, is, like Mtr, dispensable for CO-dependent, acetogenic *M. acetivorans*.

Mcr Remains Essential. Despite the fact that MKOmtrSF produced only minute amounts of methane (Fig. 2*B*), neither Mcr activity in vitro (Fig. 4*B*) nor the abundance of its subunits (*SI Appendix*, Table S6) were altered much compared to its parental strain. The presence of either BES or 3-NOP, both potent

Table 1. Growth parameters of *M. acetivorans* on CO

Strain	Growth rate [h^{-1}]	Doubling time [h]	Final OD_{578}	Yield [g/mol CO]	Yield [g/mol acetate]
M42	0.043 ± 0.002	16.0 ± 0.6	1.81 ± 0.05	2.7 ± 0.7	20.5 ± 3.6
MKOmtr3 (+2 mM MeOH)	0.040 ± 0.001	17.4 ± 0.6	1.71 ± 0.22	n.d.	n.d.
MKOmtrSF	0.040 ± 0.001	17.5 ± 0.5	1.27 ± 0.03	2.0 ± 0.6	11.2 ± 2.2
MKOmtrhdr	0.032 ± 0.001	21.6 ± 0.4	1.37 ± 0.07	2.3 ± 1.0	14.8 ± 4.1

n.d., not determined.

inhibitors of methanogenesis in vivo (27, 28) via blocking the activity of Mcr (28–30), completely abrogated growth of MKOmtrSF (*SI Appendix*, Fig. S5). Furthermore, all our efforts to delete (all or some of) the Mcr-encoding genes, *mcrBDCGA*, by using three different genetic constructs failed (*SI Appendix*, Table S7). Taken together, Mcr remains essential in MKOmtrSF—despite the fact that its energy metabolism is now acetogenic.

Discussion

Since their discovery, methanogenic microorganisms have been considered obligate methane producers (31), obviously because methane is the end product of their energy metabolism. Here, we demonstrate that a cytochrome-containing methanogen, *M. acetivorans*, is able to conserve energy and grow—in a sustained fashion—independent of methanogenesis. That the methane-releasing reaction catalyzed by Mcr remains, nonetheless, essential, we attribute to an anabolic requirement of the CoM-S-S-CoB heterodisulfide. That *M. acetivorans* can be converted from an aceto- and methylotrophic methanogen into a carboxidotrophic acetogen, solely by rewiring its endogenous metabolism (i.e., without introducing foreign genes), bears general consequence on our view of this important archaeal group.

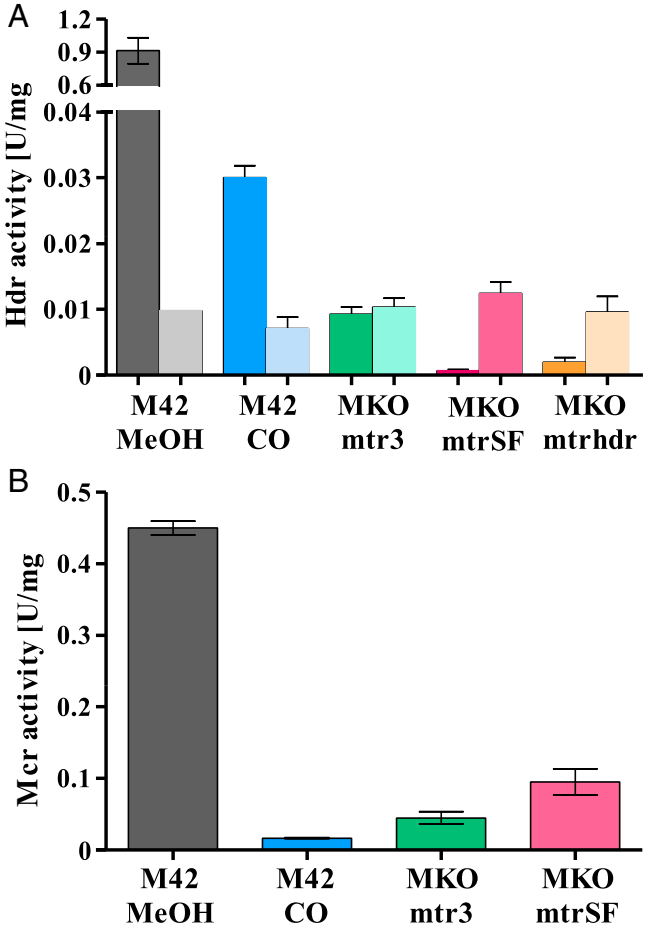

Fig. 4. Hdr and Mcr in *M. acetivorans*. Specific activity of heterodisulfide reductase (*A*) and methyl-S-CoM reductase (*B*), determined as given in *Materials and Methods*, in M42 grown on MeOH (gray), M42 grown on CO (blue), MKOmtr3 grown on CO+MeOH (1 mM) (green), MKOmtrSF grown on CO (red), and MKOmtrhdr grown on CO (yellow). (*A*) The membranous fraction is indicated by a darker shade of color, the cytoplasmic by a lighter shade of color; data shown correspond to mean values and their SD (error bars) resulting from three biological replicates, except for Hdr activity in M42 grown on MeOH, where only a single (cytoplasmic) or technical replicate (membrane) measurement is shown.

The anabolic reaction(s) in *M. acetivorans* which use(s) CoM-S-S-CoB as oxidant is/are currently unknown. It/they could follow the principle of the thiol-dependent fumarate reductase (TfrAB), which is used to provide *Methanothermobacter thermautotrophicus* with succinate for the synthesis of α-ketoglutarate (32, 33). *M. acetivorans* does not encode TfrAB and lacks this activity (*SI Appendix*, Fig. S6). Instead, its genome contains two conspicuous loci, MA4410 and MA4630-MA4631, which could be responsible for the anabolic requirement of CoM-S-S-CoB. The loci encode putative enzymes consisting of a (N-terminal domain of a) FAD/FMN-containing dehydrogenase (COG0277) and a (C-terminal domain of a) FeS cluster–containing homolog of the CoM-S-S-CoB–binding domain of Hdr, similar to TfrAB in predicted tertiary structure (*SI Appendix*, Fig. S7). Unlike the TfrAB reaction in which the thiols HS-CoM and HS-CoB serve as electron donors for fumarate reduction, MA4410 and/or MA4630-MA4631 would use CoM-S-S-CoB as an electron acceptor for an oxidation reaction. Using CoM-S-S-CoB both as the terminal catabolic as well as an anabolic electron acceptor offers a simple mechanism to integrate energy conservation and biosynthesis in *M. acetivorans* by dynamically pacing both.

The utilization of CO is energetically more favorable than that of H_2+CO_2 by alleviating the requirement of energy input for the otherwise endergonic formyl-methanofuran formation (34) (*SI Appendix*, Fig. S1). This fact might have been key for MKOmtr3 to forfeit its respiratory HdrED, and with it, catabolic methane formation, by possibly allowing to conserve energy via substrate level phosphorylation (SLP). Being able to remove HdrED raises the question about the redox cycling of the methanophenazine (MPh) pool, functioning in *Methanosarcina* analogous to quinones (*SI Appendix*, Fig. S1). It was proposed that the Rnf complex couples oxidation of reduced ferredoxin (accruing from CO oxidation) to the reduction of MPh (35–37) (*SI Appendix*, Fig. S1). The only known oxidant of reduced MPh in the respiratory chain of *Methanosarcina* is HdrED. Thus, either our understanding of the respiratory mechanism of *M. acetivorans* is incomplete, or the organism is able to thrive without MPh-dependent energetic coupling. Our experiments do not allow distinguishing between the two possibilities. Theoretically, 9 to 11 g biomass is produced per mol ATP gained through catabolism of chemotrophic anaerobes (38, 39). The biomass yield determined for MKOmtrSF of 11.2 ± 2.2 g · mol^{-1} acetate produced from CO (Table 1) is within that range. Since acetogenesis from acetyl-CoA yields 1 ATP via SLP (40), the data are consistent with MKOmtrSF growing acetogenically on CO solely via SLP. However, metabolite production from CO is not balanced for MKOmtrSF (and

MKOmtr3, respectively) (*SI Appendix*, Table S3). Unaccounted-for carbon and electrons indicate that beside the known catabolic products acetate, CO_2, and formate [methanethiol and dimethylsulfide (41) were not produced], MKOmtrSF (and MKOmtr3, respectively) generate at least one additional metabolite from—and more reduced than—CO. It is, therefore, conceivable that reoxidation of $MPhH_2$ might be coupled to the formation of (an) unknown metabolite(s). Other questions raised by the data presented here are how the strain generates methyl-S-CoM from CO in the absence of Mtr and which of the many factors lost in the strain are responsible for its dramatic phenotypic shift (*SI Appendix*, Fig. S1 and Supplementary Information Text).

Since acetogenic *M. acetivorans* MKOmtrSF was obtained solely by removing genes (and one codon of a gene, *SI Appendix*, Table S4) combined with adaptive evolution (i.e., selection-driven adjustment of the metabolic repertoire present), it is conceivable that an H_4MPT-containing acetogenic ancestor of methanogens, lacking cytochromes, Mtr, Mcr, and Hdr (and the corresponding biosynthesis and maturation machinery) (42), might have evolved methanogenesis (*SI Appendix*, Supplementary Information Text). Such a scenario would be compatible with the substantial differences in the methyl branch of the bacterial and the archaeal variant of the reductive acetyl-CoA pathway (43) and with the idea of the reductive acetyl-CoA pathway being the first metabolism (3).

Unlike other groups of chemolithotrophic microorganisms (e.g., acetogenic and sulfate-reducing bacteria) (44, 45), methanogenic archaea are metabolically very restricted, both regarding the range of electron donors they use, which include only H_2, C1 compounds, acetate, and a few secondary alcohols (31), and electron acceptors (CO_2 and methyl groups), which all lead to the formation of methane and of the CoM-S-S-CoB heterodisulfide (8). The number of experimentally validated electron donors for methanogenesis is increasing (46–48), and analyses of metagenomes even suggest sugar- and amino acid–dependent facultative methanogenic lifestyles so far not captured through cultivation (13, 49). However, alternative electron acceptors were, thus far, not reported to confer to methanogens the ability to grow nonmethanogenically in a sustained fashion (i.e., for more than a few generations). Since such ability is routinely tested by using inhibitors of Mcr, most commonly BES (50–52), the anabolic requirement of the CoM-S-S-CoB heterodisulfide (the product of the Mcr reaction) reported here may shroud the capacity of methanogens for sustained nonmethanogenic energy conservation, which might be much more extensive than currently known.

Materials and Methods

Microbiological and Molecular Methods. Standard conditions were used for plasmid constructions, growth, and transformation of *Escherichia coli* strains (53). Plasmids and strains are presented in *SI Appendix*, Table S1. *M. acetivorans* strains were grown in High-Salt (HS) medium (54, 55) or in Pipes-HS (P-HS) medium, where piperazine-*N*,*N*′-bis(2-ethanesulfonic acid) [60 mM, pH 7.4] was present. Either methanol (MeOH, 125 mM), sodium acetate (120 mM), or CO (150 kPa) served as single energy substrates for growth. 2-bromoethanesulfonate (BES, Sigma-Aldrich) and 3-nitrooxypropanol [3-NOP, synthesized at the Department of Chemistry (TU Dresden) as described (56)] were added to media from anaerobic sterile stock solutions to 5 mM and 50 μM, respectively. *M. acetivorans* was genetically manipulated as described (41, 57, 58). Growth of *M. acetivorans* in liquid cultures was monitored via its optical density (OD) at 578 nm (OD_{578}) using a spectrophotometer (Thermo Scientific) for Balch tubes or using an Ultrospec 2000 spectrophotometer (Pharmacia Biotech) for measurements of diluted culture samples. For the determination of cell yields, three replicate cultures were grown on CO in P-HS medium and passed through predried (30 min, 80 °C), weighted cellulose nitrate filters (0.45 μm pore size) (Sartorius), which were washed with 25 mL P-HS, dried at 80 °C, and weighted. CO, acetate, and CH_4 were quantified at the beginning and at the end of the experiment to derive the amounts of CO consumed and of acetate and methane formed.

Metabolite Analyses. Methane, methanethiol, and dimethylsulfide in the gas phase were quantified using a GC-2010 Plus gas chromatograph (Shimadzu GmbH) equipped with an Optima-WAXPlus column (length, 30 m; diameter, 0.32 μm; film thickness, 0.5 μm) (Macherey-Nagel) developed with N_2 or He as the carrier gas at a column flow rate of 3.39 (N_2) or 2.22 (He) ml · min^{-1}. The temperature of the flame ionization detector was set to 250 °C, that of the column oven to 40 °C, and that of the split (2:1) injector to 200 °C. CO and CO_2 in the gas phase (after acidification of the sample with 0.06 vol concentrated HCl) were quantified with the same chromatograph but using a thermal conductivity detector, which was set with a positive polarity at 80 °C, 45 mA, makeup flow 8 mL · min^{-1} for N_2 and 120 °C, 95 mA, makeup flow 7.5 mL · min^{-1} for He. The column used for this purpose was Carboxen 1010 PLOT (length, 30 m; diameter, 0.32 mm; film thickness, 15 μm) (Sigma-Aldrich), set to 80 °C, developed with N_2 or He as the carrier gas at a column flow rate of 3.8 or 3 mL · min^{-1}, respectively. The temperature of the split (5:1 for He, 2:1 for N_2) injector was set to 200 °C. Gas phase samples (50 μl) were injected with a gas-tight sample lock syringe (Hamilton). Acetate and formate in cleared supernatant samples were determined enzymatically by using an acetic or formic acid kit, respectively (R-Biopharm), and following the manufacturer's instructions.

Enzymes. All manipulations were carried out under strictly anaerobic conditions using gas-tight vials or inside an anaerobic glove box (Coy) containing N_2:H_2 (96:4 [vol/vol]). Lysates of *M. acetivorans* were prepared from cultures at exponential growth phase (OD_{578} 0.4 to 1.0) by lysing cells (sedimented by centrifugation) in the respective enzyme activity buffer for 30 min on ice. After repeated sedimentation, the supernatant represented the cleared lysate. To separate cytoplasmic and membrane fraction, cleared lysate was subjected to ultracentrifugation at 150,000 × *g* for 2 h. The resulting supernatant represented the cytoplasmic fraction. The pellet was resuspended in buffer and subjected to ultracentrifugation again. The resulting pellet represented the membrane fraction. The protein in cell fractions was quantified with the method of Bradford (59) using bovine serum albumin as standard.

Reduced viologen:CoM-S-S-CoB oxidoreductase (heterodisulfide reductase) activity was quantified in cytoplasmic and membrane fractions of *M. acetivorans* as described (60), except that the assay buffer consisted of 50 mM Tris HCl (pH 7.6) and 2 mM dithiothreitol. CoM-S-S-CoB–dependent oxidation of benzylviologen (BV) (ABCR GmbH & Co. KG) was followed at 604 nm ($\varepsilon = 10.7 \times 10^3\ M^{-1} \cdot x \cdot cm^{-1}$), and specific heterodisulfide reductase activity is expressed as units (1 U = 2 μmol BV oxidized = 1 μmol CoM-S-S-CoB reduced per min) per mg protein. The detection limit of the assay was 2 mU per mg.

Reduced viologen:fumarate oxidoreductase (fumarate reductase) activity was quantified in cleared cell lysates of *M. acetivorans* as described (33). Specific fumarate reductase activity is expressed as units (1 U = 2 μmol BV oxidized = 1 μmol fumarate reduced per min) per mg protein. The detection limit of the assay was 15 mU per mg.

For the quantification of methyl-S-CoM reductase activity in cell lysates, the described methods (61, 62) were adapted. Shortly, 0.1 mL each stock solution of CH_3-S-CoM (100 mM), CoB-S-S-CoB (5 mM), Ti(III)-citrate (200 mM), and hydroxycobalamin (3 mM) were mixed with 0.6 mL assay buffer (100 mM Tris HCl pH 7.2) before adding 0.5 mL cell lysate and incubating the reaction at 37 °C. The CH_4 produced over time was quantified by gas chromatography, and Mcr activity is given in μmol CH_4 produced per min (i.e., U) per mg protein using the average obtained from cell lysates of at least three independent cultures. The detection limit of the assay was 2 mU per mg.

Genome Analysis. For genome sequencing, DNA was isolated via the Wizard Genomic DNA Purification Kit (Promega). Illumina shotgun paired-end sequencing libraries were prepared using the Nextera XT Library Preparation Kit (Illumina) according to manufacturer's instructions and sequenced on a MiSeq instrument and the MiSeq reagent kit version 3 (2 × 300 bp) as recommended by the manufacturer (Illumina). Trimmomatic v0.39 (63) was used for quality filtering of the raw reads and Bowtie2 (64) for the mapping on the reference genome *M. acetivorans* C2A genome sequence (65) (accession no. NC_003552). The results were analyzed with Geneious Prime 2019. The raw reads of the analyzed strains have been deposited in the Sequence Read Archive (SRA) (https://www.ncbi.nlm.nih.gov/sra) under accession numbers SRR13272466 (M42) (66), SRR13272467 (MKOmtr3) (67), SRR13272468 (MKOmtrSF_I2) (68), and SRR13272469 (MKOmtrSF_I1) (69), respectively.

Proteome Analysis. A total of 1 mL exponential growing cultures were centrifuged for 10 min at 12,000 × *g* and 4 °C. After protein extraction and proteolytic cleavage, the peptide lysates were injected into nano high-performance liquid chromatograph (UltiMate 3000 RSLCnano, Dionex, Thermo Fisher Scientific). Peptide separation was performed on a C18 reverse-phase trapping column (C18 PepMap100, 300 μm × 5 mm, particle size 5 μm, nano viper, Thermo Fisher Scientific) followed by a C18 reverse-phase analytical column (Acclaim

PepMap 100, 75 μm × 25 cm, particle size 3 μm, nanoViper, Thermo Fisher Scientific). A mass spectrometric analysis of peptides was performed on a Q Exactive HF mass spectrometer (Thermo Fisher Scientific) coupled with a TriVersa NanoMate (Advion, Ltd.) source in liquid chromatography (LC) chip coupling mode. LC gradient, ionization mode, and mass spectrometry mode have been used as described (70). Raw data were processed with Proteome Discoverer (v2.2, Thermo Fisher Scientific). Search settings for the Sequest HT search engine were set to trypsin (Full), max. missed cleavage: 2, precursor mass tolerance: 10 ppm, fragment mass tolerance: 0.02 Da. The raw files were searched against the protein-coding sequences of *M. acetivorans*. Peptides representing proteins eliminated through targeted (Hpt in all strains, MtrEDCBAFGH in MKOmtr3 and MKOmtrSF) or spontaneous mutation(s) (MA2190-MA2335 in MKOmtrSF) were discarded, as they are not present in the respective strain. The false discovery rates (FDR) were determined with the node Percolator (71) embedded in Proteome Discoverer and were set to the FDR threshold at a peptide and protein level of 0.01. Protein grouping was performed according to strict parsimony principle. The individual protein abundances were $\log_2$ transformed and normalized using medians. Differences were defined as significant with a threshold of ± 2.5-fold difference in abundance. Proteins, which are identifiable only via one unique peptide, were only scored as absent when the peptide could not be found in all five replicates of the respective strain. The mass spectrometry proteomics data have been deposited to the ProteomeXchange Consortium via the PRIDE (72) (https://www.ebi.ac.uk/pride/) partner repository with the dataset identifier PXD022016 (73).

Data Availability. Raw sequencing reads and mass spectrometry proteomics data have been deposited in SRA and PRIDE (SRR13272466–SRR13272469, and PXD022016). All other study data are included in the article and/or *SI Appendix*.

ACKNOWLEDGMENTS. We thank Seigo Shima (Marburg) and Uwe Deppenmeier (Bonn) for generously providing CoM-S-S-CoB, Johannes Finke (Frankfurt) for help during cloning procedures, and Ivan Berg (Münster) for critical reading of the manuscript. M.V. and N.J. acknowledge support from the Helmholtz Centre for Environmental Research for the ProMetheus platform for proteomics and metabolomics. This work was supported by grants from the Graduate Academy of the Technische Universität Dresden to C.S., Novo Nordisk Foundation Grant NNF19OC0055464 to N.A., and Academy of Finland Grant 326020 to S.S.

1. C. Huber, G. Wächtershäuser, Activated acetic acid by carbon fixation on (Fe,Ni)S under primordial conditions. *Science* **276**, 245–247 (1997).
2. M. Preiner *et al.*, A hydrogen-dependent geochemical analogue of primordial carbon and energy metabolism. *Nat. Ecol. Evol.* **4**, 534–542 (2020).
3. W. F. Martin, Older than genes: The acetyl CoA pathway and origins. *Front. Microbiol.* **11**, 817 (2020).
4. L. G. Ljungdahl, The autotrophic pathway of acetate synthesis in acetogenic bacteria. *Annu. Rev. Microbiol.* **40**, 415–450 (1986).
5. A. Y. Sun, L. Ljungdahl, H. G. Wood, Total synthesis of acetate from CO_2. II. Purification and properties of formyltetrahydrofolate synthetase from *Clostridium thermoaceticum*. *J. Bacteriol.* **98**, 842–844 (1969).
6. K. Schuchmann, V. Müller, Autotrophy at the thermodynamic limit of life: A model for energy conservation in acetogenic bacteria. *Nat. Rev. Microbiol.* **12**, 809–821 (2014).
7. J. C. Escalante-Semerena, K. L. Rinehart Jr., R. S. Wolfe, Tetrahydromethanopterin, a carbon carrier in methanogenesis. *J. Biol. Chem.* **259**, 9447–9455 (1984).
8. R. K. Thauer, A. K. Kaster, H. Seedorf, W. Buckel, R. Hedderich, Methanogenic archaea: Ecologically relevant differences in energy conservation. *Nat. Rev. Microbiol.* **6**, 579–591 (2008).
9. D. Möller-Zinkhan, R. K. Thauer, Anaerobic lactate oxidation to 3 CO_2 by *Archaeoglobus fulgidus* via the carbon monoxide dehydrogenase pathway: Demonstration of the acetyl-CoA carbon-carbon cleavage reaction in cell extracts. *Arch. Microbiol.* **153**, 215–218 (1990).
10. P. G. Simpson, W. B. Whitman, "Anabolic pathways in methanogens" in *Methanogenesis*, J. G. Ferry, Ed. (Springer, New York, 1993), pp. 445–472.
11. M. Rother, W. W. Metcalf, Anaerobic growth of *Methanosarcina acetivorans* C2A on carbon monoxide: An unusual way of life for a methanogenic archaeon. *Proc. Natl. Acad. Sci. U.S.A.* **101**, 16929–16934 (2004).
12. A. M. Henstra, C. Dijkema, A. J. Stams, *Archaeoglobus fulgidus* couples CO oxidation to sulfate reduction and acetogenesis with transient formate accumulation. *Environ. Microbiol.* **9**, 1836–1841 (2007).
13. P. N. Evans *et al.*, Methane metabolism in the archaeal phylum Bathyarchaeota revealed by genome-centric metagenomics. *Science* **350**, 434–438 (2015).
14. S. Suzuki, K. H. Nealson, S. Ishii, Genomic and *in-situ* transcriptomic characterization of the Candidate Phylum NPL-UPL2 from highly alkaline highly reducing serpentinized groundwater. *Front. Microbiol.* **9**, 3141 (2018).
15. W. D. Orsi *et al.*, Metabolic activity analyses demonstrate that Lokiarchaeon exhibits homoacetogenesis in sulfidic marine sediments. *Nat. Microbiol.* **5**, 248–255 (2020).
16. B. Becher, V. Müller, G. Gottschalk, *N5*-methyl-tetrahydromethanopterin: Coenzyme M methyltransferase of *Methanosarcina* strain Gö1 is an $Na(^+)$-translocating membrane protein. *J. Bacteriol.* **174**, 7656–7660 (1992).
17. U. Ermler, W. Grabarse, S. Shima, M. Goubeaud, R. K. Thauer, Crystal structure of methyl-coenzyme M reductase: The key enzyme of biological methane formation. *Science* **278**, 1457–1462 (1997).
18. K. Raymann, C. Brochier-Armanet, S. Gribaldo, The two-domain tree of life is linked to a new root for the Archaea. *Proc. Natl. Acad. Sci. U.S.A.* **112**, 6670–6675 (2015).
19. G. Borrel, P. S. Adam, S. Gribaldo, Methanogenesis and the Wood-Ljungdahl pathway: An ancient, versatile, and fragile association. *Genome Biol. Evol.* **8**, 1706–1711 (2016).
20. B. A. Berghuis *et al.*, Hydrogenotrophic methanogenesis in archaeal phylum Verstraetearchaeota reveals the shared ancestry of all methanogens. *Proc. Natl. Acad. Sci. U.S.A.* **116**, 5037–5044 (2019).
21. B. Becher, V. Müller, G. Gottschalk, The methyl-tetrahydromethanopterin: Coenzyme M methyltransferase of *Methanosarcina* strain Gö1 is a primary sodium pump. *FEMS Microbiol. Lett.* **91**, 239–243 (1992).
22. D. J. Lessner *et al.*, An unconventional pathway for reduction of CO_2 to methane in CO-grown *Methanosarcina acetivorans* revealed by proteomics. *Proc. Natl. Acad. Sci. U.S.A.* **103**, 17921–17926 (2006).
23. P. V. Welander, W. W. Metcalf, Loss of the *mtr* operon in *Methanosarcina* blocks growth on methanol, but not methanogenesis, and reveals an unknown methanogenic pathway. *Proc. Natl. Acad. Sci. U.S.A.* **102**, 10664–10669 (2005).
24. J. T. Keltjens, G. D. Vogels, "Conversion of methanol and methylamines to methane and carbon dioxide" in *Methanogenesis*, J. G. Ferry, Ed. (Springer, New York, 1993), pp. 253–303.
25. D. R. Lasko, C. Schwerdel, J. E. Bailey, U. Sauer, Acetate-specific stress response in acetate-resistant bacteria: An analysis of protein patterns. *Biotechnol. Prog.* **13**, 519–523 (1997).
26. N. R. Buan, W. W. Metcalf, Methanogenesis by *Methanosarcina acetivorans* involves two structurally and functionally distinct classes of heterodisulfide reductase. *Mol. Microbiol.* **75**, 843–853 (2010).
27. W. E. Balch, R. S. Wolfe, Specificity and biological distribution of coenzyme M (2-mercaptoethanesulfonic acid). *J. Bacteriol.* **137**, 256–263 (1979).
28. E. C. Duin *et al.*, Mode of action uncovered for the specific reduction of methane emissions from ruminants by the small molecule 3-nitrooxypropanol. *Proc. Natl. Acad. Sci. U.S.A.* **113**, 6172–6177 (2016).
29. R. P. Gunsalus, J. A. Romesser, R. S. Wolfe, Preparation of coenzyme M analogues and their activity in the methyl coenzyme M reductase system of *Methanobacterium thermoautotrophicum*. *Biochemistry* **17**, 2374–2377 (1978).
30. M. Goenrich *et al.*, Probing the reactivity of Ni in the active site of methyl-coenzyme M reductase with substrate analogues. *J. Biol. Inorg. Chem.* **9**, 691–705 (2004).
31. W. B. Whitman, T. L. Bowen, D. R. Boone, "The methanogenic bacteria" in *The Prokaryotes—A Handbook on the Biology of Bacteria*, M. Dworkin *et al.*, Eds. (Springer, New York, **vol. 3**, 2006), pp. 165–207.
32. T. A. Bobik, R. S. Wolfe, An unusual thiol-driven fumarate reductase in *Methanobacterium* with the production of the heterodisulfide of coenzyme M and N-(7-mercaptoheptanoyl)threonine-*O3*-phosphate. *J. Biol. Chem.* **264**, 18714–18718 (1989).
33. S. Heim, A. Künkel, R. K. Thauer, R. Hedderich, Thiol: Fumarate reductase (Tfr) from *Methanobacterium thermoautotrophicum*–Identification of the catalytic sites for fumarate reduction and thiol oxidation. *Eur. J. Biochem.* **253**, 292–299 (1998).
34. A. Stojanowic, R. Hedderich, CO_2 reduction to the level of formylmethanofuran in *Methanosarcina barkeri* is non-energy driven when CO is the electron donor. *FEMS Microbiol. Lett.* **235**, 163–167 (2004).
35. Q. Li *et al.*, Electron transport in the pathway of acetate conversion to methane in the marine archaeon *Methanosarcina acetivorans*. *J. Bacteriol.* **188**, 702–710 (2006).
36. M. Wang, J. F. Tomb, J. G. Ferry, Electron transport in acetate-grown *Methanosarcina acetivorans*. *BMC Microbiol.* **11**, 165 (2011).
37. S. Suharti, M. Wang, S. de Vries, J. G. Ferry, Characterization of the RnfB and RnfG subunits of the Rnf complex from the archaeon *Methanosarcina acetivorans*. *PLoS One* **9**, e97966 (2014).
38. T. Bauchop, S. R. Elsden, The growth of micro-organisms in relation to their energy supply. *J. Gen. Microbiol.* **23**, 457–469 (1960).
39. K. Decker, K. Jungermann, R. K. Thauer, Energy production in anaerobic organisms. *Angew. Chem. Int. Ed. Engl.* **9**, 138–158 (1970).
40. R. K. Thauer, K. Jungermann, K. Decker, Energy conservation in chemotrophic anaerobic bacteria. *Bacteriol. Rev.* **41**, 100–180 (1977).
41. E. Oelgeschläger, M. Rother, *In vivo* role of three fused corrinoid/methyl transfer proteins in *Methanosarcina acetivorans*. *Mol. Microbiol.* **72**, 1260–1272 (2009).
42. A. K. Kaster *et al.*, More than 200 genes required for methane formation from H_2 and CO_2 and energy conservation are present in *Methanothermobacter marburgensis* and *Methanothermobacter thermautotrophicus*. *Archaea* **2011**, 973848 (2011).
43. F. L. Sousa, W. F. Martin, Biochemical fossils of the ancient transition from geoenergetics to bioenergetics in prokaryotic one carbon compound metabolism. *Biochim. Biophys. Acta* **1837**, 964–981 (2014).
44. G. Muyzer, A. J. Stams, The ecology and biotechnology of sulphate-reducing bacteria. *Nat. Rev. Microbiol.* **6**, 441–454 (2008).

45. K. Schuchmann, V. Müller, Energetics and application of heterotrophy in acetogenic bacteria. *Appl. Environ. Microbiol.* **82**, 4056–4069 (2016).
46. A. K. Bock, A. Priegerkraft, P. Schönheit, Pyruvate – A novel substrate for growth and methane formation in *Methanosarcina barkeri. Arch. Microbiol.* **161**, 33–46 (1994).
47. T. Uchiyama, K. Ito, K. Mori, H. Tsurumaru, S. Harayama, Iron-corroding methanogen isolated from a crude-oil storage tank. *Appl. Environ. Microbiol.* **76**, 1783–1788 (2010).
48. S. T. Lohner, J. S. Deutzmann, B. E. Logan, J. Leigh, A. M. Spormann, Hydrogenase-independent uptake and metabolism of electrons by the archaeon *Methanococcus maripaludis. ISME J.* **8**, 1673–1681 (2014).
49. I. Vanwonterghem *et al.*, Methylotrophic methanogenesis discovered in the archaeal phylum Verstraetearchaeota. *Nat. Microbiol.* **1**, 16170 (2016).
50. A. K. Bock, P. Schönheit, Growth of *Methanosarcina barkeri* (Fusaro) under nonmethanogenic conditions by the fermentation of pyruvate to acetate: ATP synthesis via the mechanism of substrate level phosphorylation. *J. Bacteriol.* **177**, 2002–2007 (1995).
51. D. Prakash, S. S. Chauhan, J. G. Ferry, Life on the thermodynamic edge: Respiratory growth of an acetotrophic methanogen. *Sci. Adv.* **5**, eaaw9059 (2019).
52. D. E. Holmes *et al.*, A membrane-bound cytochrome enables *Methanosarcina acetivorans* to conserve energy from extracellular electron transfer. *MBio* **10**, e00789-19 (2019).
53. F. M. Ausubel *et al.*, Eds., *Current Protocols in Molecular Biology* (J. Wiley & Sons, Inc., New York, 2003).
54. K. R. Sowers, J. E. Boone, R. P. Gunsalus, Disaggregation of *Methanosarcina* spp. and growth as single cells at elevated osmolarity. *Appl. Environ. Microbiol.* **59**, 3832–3839 (1993).
55. K. R. Sowers, K. M. Noll, "Techniques for anaerobic growth" in *Methanogens*, K. R. Sowers, H. J. Schreier, Eds. (Cold Spring Harbor Laboratory Press, Plainview, NY, **vol. 2**, 1995), pp. 15–47.
56. M. Biava *et al.*, Novel analgesic/anti-inflammatory agents: Diarylpyrrole acetic esters endowed with nitric oxide releasing properties. *J. Med. Chem.* **54**, 7759–7771 (2011).
57. W. W. Metcalf, J. K. Zhang, E. Apolinario, K. R. Sowers, R. S. Wolfe, A genetic system for Archaea of the genus *Methanosarcina*: Liposome-mediated transformation and construction of shuttle vectors. *Proc. Natl. Acad. Sci. U.S.A.* **94**, 2626–2631 (1997).
58. P. Boccazzi, J. K. Zhang, W. W. Metcalf, Generation of dominant selectable markers for resistance to pseudomonic acid by cloning and mutagenesis of the *ileS* gene from the archaeon *Methanosarcina barkeri* fusaro. *J. Bacteriol.* **182**, 2611–2618 (2000).
59. M. M. Bradford, A rapid and sensitive method for the quantitation of microgram quantities of protein utilizing the principle of protein-dye binding. *Anal. Biochem.* **72**, 248–254 (1976).
60. R. Hedderich, A. Berkessel, R. K. Thauer, Catalytic properties of the heterodisulfide reductase involved in the final step of methanogenesis. *FEBS Lett.* **255**, 67–71 (1989).
61. L. G. Bonacker, S. Baudner, E. Mörschel, R. Böcher, R. K. Thauer, Properties of the two isoenzymes of methyl-coenzyme M reductase in *Methanobacterium thermoautotrophicum. Eur. J. Biochem.* **217**, 587–595 (1993).
62. S. Scheller, M. Goenrich, R. K. Thauer, B. Jaun, Methyl-coenzyme M reductase from methanogenic archaea: Isotope effects on the formation and anaerobic oxidation of methane. *J. Am. Chem. Soc.* **135**, 14975–14984 (2013).
63. A. M. Bolger, M. Lohse, B. Usadel, Trimmomatic: A flexible trimmer for Illumina sequence data. *Bioinformatics* **30**, 2114–2120 (2014).
64. B. Langmead, S. L. Salzberg, Fast gapped-read alignment with Bowtie 2. *Nat. Methods* **9**, 357–359 (2012).
65. J. E. Galagan *et al.*, The genome of *M. acetivorans* reveals extensive metabolic and physiological diversity. *Genome Res.* **12**, 532–542 (2002).
66. Georg-August-University Goettingen, MEAM7. Sequence Read Archive. https://www.ncbi.nlm.nih.gov/sra/?term=SRR13272466. Deposited 18 December 2020.
67. Georg-August-University Goettingen, MEAM3. Sequence Read Archive. https://www.ncbi.nlm.nih.gov/sra/?term=SRR13272467. Deposited 18 December 2020.
68. Georg-August-University Goettingen, MEAM8. Sequence Read Archive. https://www.ncbi.nlm.nih.gov/sra/?term=SRR13272468. Deposited 18 December 2020.
69. Georg-August-University Goettingen, MEAM4. Sequence Read Archive. https://www.ncbi.nlm.nih.gov/sra/?term=SRR13272469. Deposited 18 December 2020.
70. S. B. Haange *et al.*, Disease development is accompanied by changes in bacterial protein abundance and functions in a refined model of dextran sulfate sodium (DSS)-induced colitis. *J. Proteome Res.* **18**, 1774–1786 (2019).
71. L. Käll, J. D. Canterbury, J. Weston, W. S. Noble, M. J. MacCoss, Semi-supervised learning for peptide identification from shotgun proteomics datasets. *Nat. Methods* **4**, 923–925 (2007).
72. Y. Perez-Riverol *et al.*, The PRIDE database and related tools and resources in 2019: Improving support for quantification data. *Nucleic Acids Res.* **47**, D442–D450 (2019).
73. N. Jehmlich, PXD022016, Proteomics Identifications Database. https://www.ebi.ac.uk/pride/archive/projects/PXD022016. Deposited 16 October 2020.